Journal of the European Ceramic Society 21 (2001) 105–118

www.elsevier.com/locate/jeurceramsoc

Biomorphous ceramics from lignocellulosics

Peter Greil

University of Erlangen-Nuernberg, Department of Materials Science (III), Erlangen, Germany

Received 30 March 2000; received in revised form 26 May 2000; accepted 4 June 2000

Abstract

Lignocellulosics represent the organic matter produced by trees. Biopolymers such as cellulose, hemicellulose and lignin are the major macromolecular constituents of ligneous cell walls which are distinguished by a hierarchical fibrilar composite micro structure. Fundamental aspects of anatomy of wood and molecular structure of wood cell wall affecting the bioorganic–inorganic conversion process are reviewed. Basic approaches to convert the native biopolymeric materials into non-oxide as well as oxide ceramic products include: (i) pyrolytic decomposition resulting in a porous carbon replica (template) which may subsequently be reacted to form carbide phases or may be infiltrated with non-reacting sols or salts which can further be processed to yield oxide reaction products; (ii) infiltration of chemically preprocessed native lignocellulosic products with gaseous or liquid organometallic and metalorganic precursors and subsequent oxidation to remove the free carbon phase. Conversion of native (wood tissue) lignocellulosics into ceramics with a microstructure pseudomorphous to the bioorganic template anatomy offers a great potential for designing novel ceramics with anisotropic cellular morphologies. These might be of interest for applications as high temperature resistant exhaust gas filters and catalyst carriers in energy, environmental and automotive industries, bioinert and corrosion resistant immobilization supports for living cells, microbes, or enzymes in biotechnology and medicine.

Keywords: Biomimetics; Lignocellusosics; Wood-ceramics

1. Introduction

Lignocellulosics from the class of organic matter produced by land-growing plants in the form of trees, shrubs, and agricultural crops. It is the essential carbon sink on the planet which is formed by catalytic conversion of carbon dioxide to an organic mass mainly consisting of the elements C–O(–N)–H. Lignocellulosic biocomposites are intricate materials with great biodiversity, but with chemical compositions that make use of only minor variations of principally two different monomeric repeat units: mono-saccharides (pentoses and hexoses) forming celluloses and hemicelluloses, and *p*-OH phenylpropanes present in lignin. Cellulose-rich fibers are separated, isolated, and purified by aqueous delignification and mild hydrolysis in an acidic or alkaline medium which is the only large scale chemical technology dealing with lignocellulosics.[1] Major products are paper and pulp and only a minor part of isolated cellulose is dedicated for fiber and cellulose derivatives (carboxymethylcellulose, cellulose acetate) production. Future activities are expected to make use of lignocellulosics as an alternative source of biobased polymers for use in structural materials. Biopolymers are abundant, renewable, biodegradable, and recycleable.

Design of novel ceramic structures by mimicking the cellular tissue anatomy of native lignocellulosic structures such as wood, fibers, surfaces of leafs, etc. has recently attained increasing interest.[2–5] For example, anti-adhesive plant surfaces caused by different cuticular microstructures (trichomes, cuticular folds, wax crystals) were analyzed[6] in order to generate self-cleaning, water-repellent surfaces (*Lotus effect*). Another example is the formation of Al_2O_3,[7] TiO_2,[8] SiC and Si_3N_4 fibers[9] from natural fibers such as sisal, jute, hemp, or cotton, and SiC whiskers from rice husks and coconut shells.[10–12] The highly anisotropic cellular structure of wood may serve as a hierarchical template to generate novel cellular ceramics with a micro-, meso- and macro-structure pseudomorphous to the initial porous tissue skeleton ranging from nanometers (cell wall fibrils) to milimeters (growth ring patterns).[3–5,13]

E-mail address: greil@ww.uni-erlangen.de

0955-2219/01/$ - see front matter
PII: S0955-2219(00)00179-5

Wood typically contains 10–20 wt.% of hemicellulose, 10–30 wt.% of lignin, and 30–55 wt.% of cellulose (and less than 2 wt.% of ash including minerals).[14] Previous work on converting wood into ceramic focused on liquid infiltration of the pyrolysed carbon template with sols of tetraethylorthosilicate (TEOS) at low temperature[3] or silicon melt at high temperatures.[14,15] Subsequently, the infiltrant was converted into SiC by pyrolysis in inert atmosphere (TEOS) or reaction with carbon (silicon). A variety of different kinds of wood such as oak (*Quercus robur*), maple (*Acer pseudoplatanus*), beech (*Fagus sylvatica*), ebony (*Diospyros celebica*), balsa (*Ochroma pyramidale*), and pine (*Pinus sylvestris*) were converted to isomorphous cellular silicon carbide ceramics.[4,13] Due to the uniaxial pore channel orientation pronounced anisotropic differences of mechanical properties e.g. strength, elastic modulus, failure strain, fracture patterns were found. Generally, the mechanical properties scale by a power law of 2nd or 3rd order with fractional density.[15] Properties in axial direction (parallel to the trunk axis) of SiC ceramics pseudomorphous to wood were found to attain significantly higher values compared to the tangential and radial loading directions.[13]

Biomophous ceramics with the cellular structure of the native or preprocessed lignocellulosics precursor but consisting of high temperature and corrosion resistant ceramic compounds such as carbides, nitrides, oxides, etc. are of particular interest because:

- native tissue is supposed to be in a mechanical state of equilibrium optimally adopted to the external loading situation during growth;
- native tissue exhibits unique structural features such as hierarchy, selectivity and anisotropy combined in the cellular anatomy;
- native tissue is available in an almost infinite diversity and variety of structures;
- growth of natural plants can be manipulated by chemical and physical methods in order to tailor tissue structures with optimized functionality e.g. pore size distribution, strut thickness, etc.;
- preprocessing of lignocellulosics by delignification and surface treatment of cellulose fibers offers a versatile pool of cellulose fiber macrostructures to be used for manufacturing of light weight ceramic structures.

Cellular ceramics with homogeneous (monomodal) or heterogenous (multimodal or fractal) anisotropic pore structures might be of interest for high temperature resistant exhaust gas filters and catalyst carriers in energy and environmental technology, bioinert and corrosion resistant immobilization supports for living cells, microbes, or enzymes in medicine and biotechnology, etc.

While previous work on "*ceramic wood*" was focused on converting native wood or a pyrolyzed carbon template primarily into SiC[3–5] fundamental questions remain to be addressed for future development of products. For example, conversion processes have to be developed which allow manufacturing of oxide ceramics of variable composition. An adequate chemical pretreatment of lignocellulosics is necessary to reduce shrinkage and to achieve net shape conversion of complex structures. Structural limitations with respect to size and shape of pores and cell wall structures have to be identified and the effects of non-uniformity of native cellular structures on property variations have to be examined.

In the following, basic principles of conversion of lignocellulosics into ceramic structures mimicking the initial precursor structure at various hierarchical micro- and macro structural levels, will be discussed. Fundamental aspects of the anatomy of wood and the molecular structure of wood cell wall affecting the bioorganic–inorganic conversion process are reviewed.

Basic approaches to convert the native biopolymeric materials into non-oxide as well as oxide ceramic products include:

(i) pyrolytic decomposition resulting in a porous carbon replica (template) which may subsequently be reacted to form carbide phases or may be infiltrated with non- reacting sols or salts which can further be processed to yield oxide reaction products;
(ii) infiltration of chemically preprocessed native or technical lignocellulosic products with gaseous or liquid organometallic and metalorganic precursors and subsequent oxidation to remove free carbon phase.

Conversion of native (wood tissue) lignocellulosics into ceramics with a microstructure pseudomorphous to the bioorganic template anatomy offers a great potential for designing novel ceramics with anisotropic cellular morphologies.

2. Anatomy of wood

Wood is a naturally grown composite material of complex hierarchical cellular structure.[16] Both hardwoods (deciduous wood which is botanically classified as *dicotlyedonous angiosperms*) and softwoods (coniferous wood or *gymnosperms*) are comprised of elongated tubular cells (sclerenchyma cells) aligned with the axis of the tree trunk. Fig. 1 shows some examples of native wood tissue with different pore structures in the axial direction (axial cross section). Vessel elements (tracheas), also called "pores", are typical for hardwoods

and may be distributed in cross-sections in either ring porous, semi-ring porous, or diffusive porous patterns. Other cell types are present, notably fibers (thick-walled mechanical support cells), ray parenchyma (small, thin-walled food transport and storage cells), and axial parenchyma (food storage cells which are vertically elongated in a standing tree stem). The size of these cells and their distribution varies considerably among different species of wood as well as among trees of a given species and within a single tree.[17] Softwoods are less complicated anatomically than hard-woods because they contain fewer cell types with less variation in the size and arrangement of those cell types in the wood structure. They do not have the vessel elements and a single cell type, the longitudinal tracheid, constitutes more than 90% of the volume of most types of softwood. These longitudinal tracheids (known as "fibers" in industry and commerce) are considerably longer (3–5 mm) and have a larger diameter (30–45 μm) than their counterpart in hard-woods which show a shorter extension of 0.1–0.8 mm but larger diameters of 10–400 μm. Softwoods can be categorized by the presence or absence of resin canals and the distinctivness of the latewood portion of a growth ring (abrupt or gradual transition of lumen diameter and cell wall thickness). Fig. 2 shows the major structural features of wood tissue resulting from cambial growth process.

Hard wood such as oak has an average composition of cellulose (40–50 wt.%), hemicellulose (20–35 wt.%), and lignin (15–35 wt.%). The molecular structures and compositions of the major biopolymers cellulose, hemicellulose and lignin are complex and may vary for different kinds of wood. Chemically the major constituents of wood are C (50 wt.%), O (44 wt.%) and H (6 wt.%) and trace elements (1 wt.%). On the micro scale wood tracheid vessels are hollow tubes made up of several concentric layers each layer being reinforced by helical macrofibrils of cellulose. The fiber orientation in the cell wall exerts a strong influence on the shrinkage behavior and its mechanical properties of wood.[16,18] Tensile modulus of hard woods may vary between 30 and 250 MPa.

From an application point of view, native cellular structures may be divided into homogenous and heterogenous structures characterized by a monomodal or a multimodal cell size distribution, respectively. Fig. 3 shows the pore channel diameter distribution of oak and pine as derived from mercury intrusion experiments and stereological analysis of cross sectional images. Interconnectivity is another feature to differentiate tissue anatomy with respect to permeability for fluid media. The fiber volume in hard wood like oak may average 50 vol.% of the biomass volume and the large diameter vessel elements are joined endwise to form tubes along the trunk or branch. The interconnective pore system of native wood provides an excellent accessibility for infiltration fluids via the inherent vascular transportation system (xylem).[19]

For native wood a model for the cellular microstructure was derived by Gibson and Ashby[15] which relates the fractional density with the anatomical features of prismatic pore edge length, l, and strut thickness, t,

$$\rho_{\mathrm{rel}} = \frac{\rho_{\mathrm{geo}}}{\rho_{\mathrm{strut}}} = \frac{2t}{\sqrt{3}l}\left(1 - \frac{t}{2\sqrt{3}l}\right) \quad (1)$$

Using the microstructure model, the mechanical behavior of cellular materials like wood tissue was described by a power law function of ρ_{rel}

$$E^* = \frac{E_{\mathrm{porous}}}{E_{\mathrm{dense}}} = C\rho_{\mathrm{rel}}^n \quad (2)$$

where E^* represents the fractional property with respect to the fully dense material (Young's modulus, shear modulus, tensile modulus, Poisson constant, fracture toughness, etc.), C is a constant and n depends on the property and the loading direction and may typically attain values between 1 and 5.[15]

Cellular anatomy of the woody tissue can be influenced by changing the cambial activity and xylogenesis during growth. In the presence of specific phytohormones for example auxine, abscisin acid, gibberilin, cell differentiation during growth can be modified. Thus, cell dimensions e.g. diameter of lumen and cell wall thickness may be altered as well as the seasonal variations e.g. early to late wood growth ring patterns.[20,21] Applying mechanical stress during growth is another method to stimulate formation of reaction tissue which may differ significantly from the regular tissue. For example growth of beech under compression resulted in a cellular anatomy where no vessels were formed whereas in unconstrained grown beech large vessels are present.[22]

3. Molecular structure of wood cell wall

While the anatomical differences in gross cellular structure between different kinds of wood (both hard- and softwoods) can be very large, the general structure of the cell wall is relatively consistent. A single longitudinal tracheid exhibits a layered wall structure, a thin primary (first-formed) wall and a thicker secondary wall composed of three sublayers known as S1, S2, and S3 layers, Fig. 4. The basic framework of each secondary wall layer (S1–S3) consists of cellulose with varying amounts of hemicellulose, pectin and lignin. Adjacent tracheids are joined together by a highly lignified layer (middle lamella). The composition of the multiphase cell wall can be likened to a fiber reinforced organic glass where cellulose serves as lightweight fiber, lignin serves

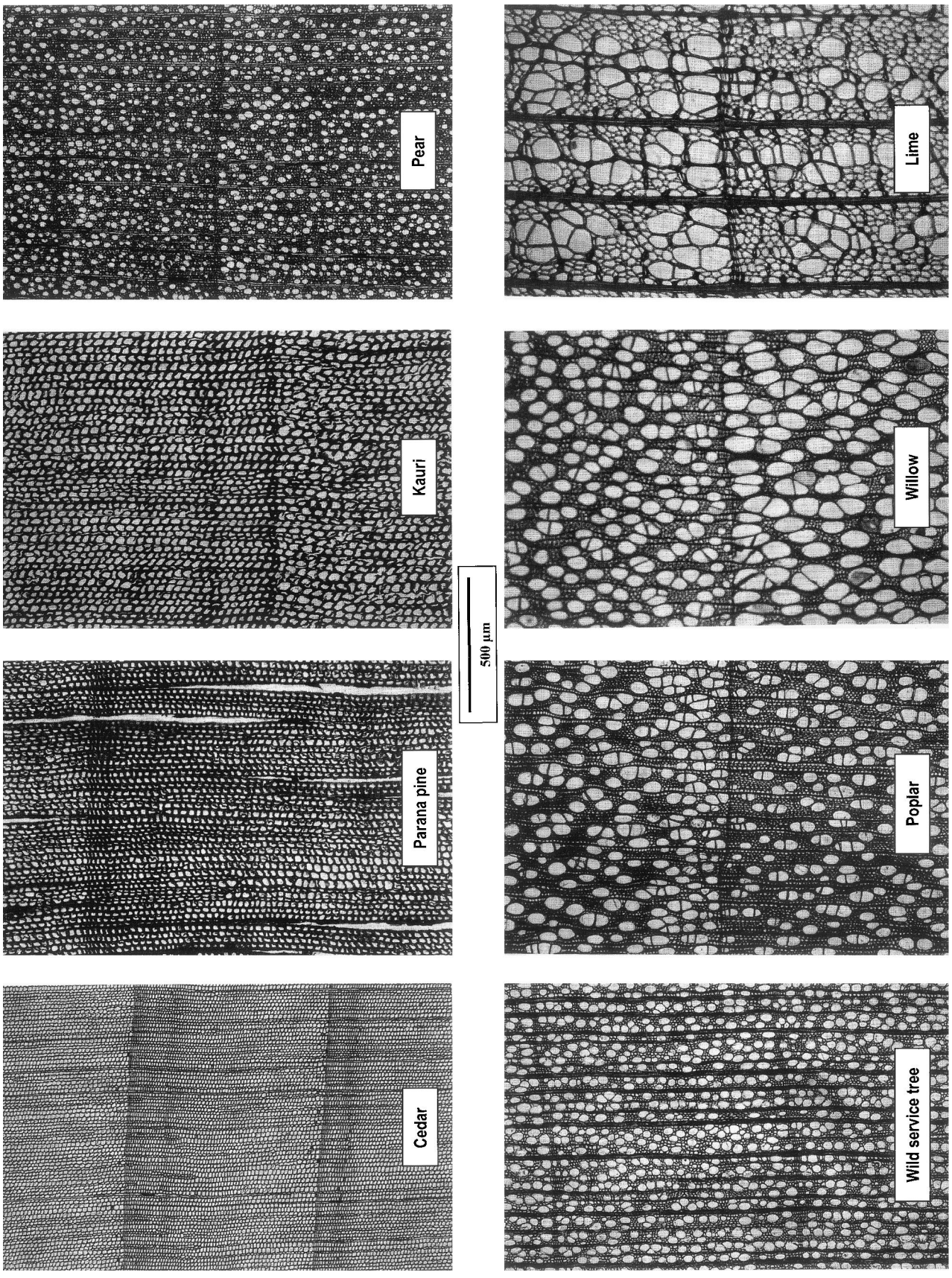

Fig. 1. Selection of tissue anatomies of various kinds of wood showing the variability of tracheidal pore structure (axial cross-section).[14]

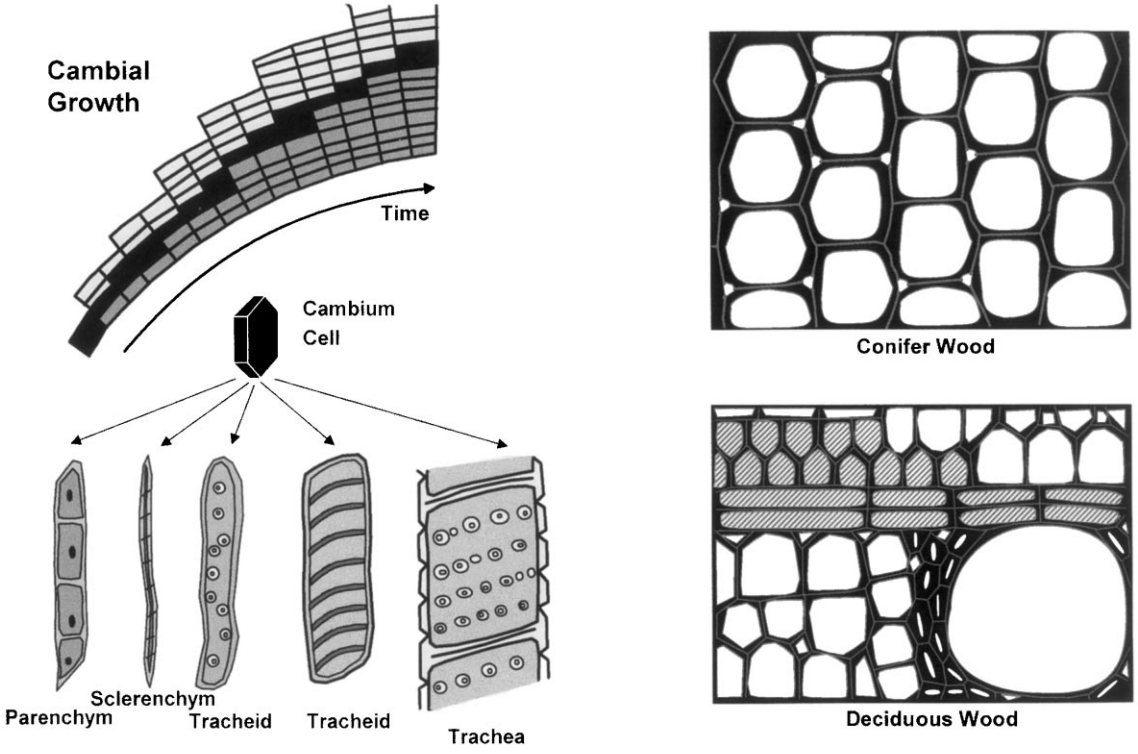

Fig. 2. Basic features of cell differentiation resulting from growth processes in native wood.

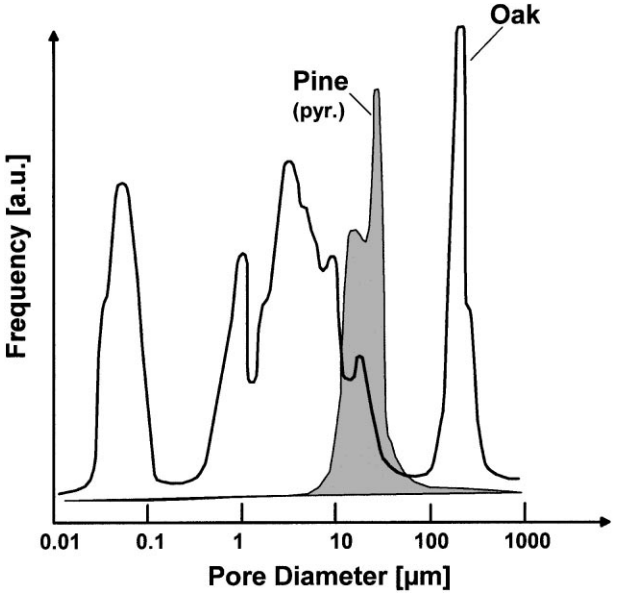

Fig. 3. Pore size distribution of a coniferous (pine) and a deciduous (oak) wood showing multimodal and monomodal nature of axial cellular porosity.

as a continous (glassy) matrix, and hemicelluloses and pectin serve as coupling agents. Fig. 5 shows the basic features of the molecular structures of the major biopolymers forming the native cell wall.

Cellulose is the key polymeric component in the structure of the cell wall. It is a long-chain linear condensation polymer (chain length up to 1 μm for native plant cellulose) of β-D-glucose with three free hydroxyl groups on each monomeric unit, resulting in strong inter- and intramolecular hydrogen bonds. Because of the hydrogen bond network, and also due to the restricted rotation around the polymeric 1,4-β-linkage, cellulose is a rigid and stiff chain providing mechanical stability to the cell wall. Due to the intermolecular hydrogen bonds in cellulose coupled with the inherent stiffness of the polymeric chains, high levels of crystallinity are found.[23,24] The cellulose molecules aggregate into microfibrils, whose orientation angle between fiber elongation and axial cell direction varies in the different cell wall layers: primary layer with a random interwoven network; secondary layers S1 :0.1–0.2 μm with $\vartheta = 50–70°$, S2: several μm with $\vartheta = 5–20°$ and S3: $\vartheta = 60–90°$.[25]

Hemicellulose is a generic term for the various polysaccharides other than cellulose found in native plants. The chemical composition of hemicelluloses is extraordinarily similar to cellulose (polyanhydro-pyranoside e.g. polymers of various pentoses such as xylose, arabinose, and hexoses like glucose, mannose, galactose, etc.), but their morphological structure is vastly different.[26] The degree of polymerization of hemicellulose is about an order of magnitude less than that of cellulose.

Pectin is a generic term for a group of polysaccharides characterized by high uronic acid content, the presence of methyl esther groups, and frequently a measurable

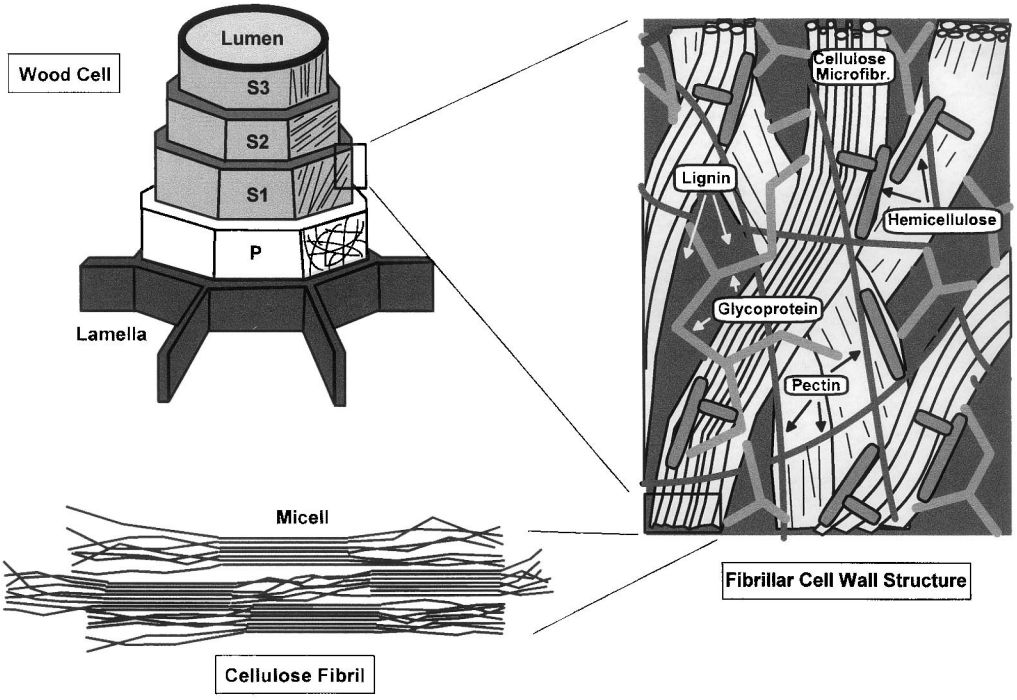

Fig. 4. Hierarchical anatomy of a wood cell and its major biopolymer constituents.

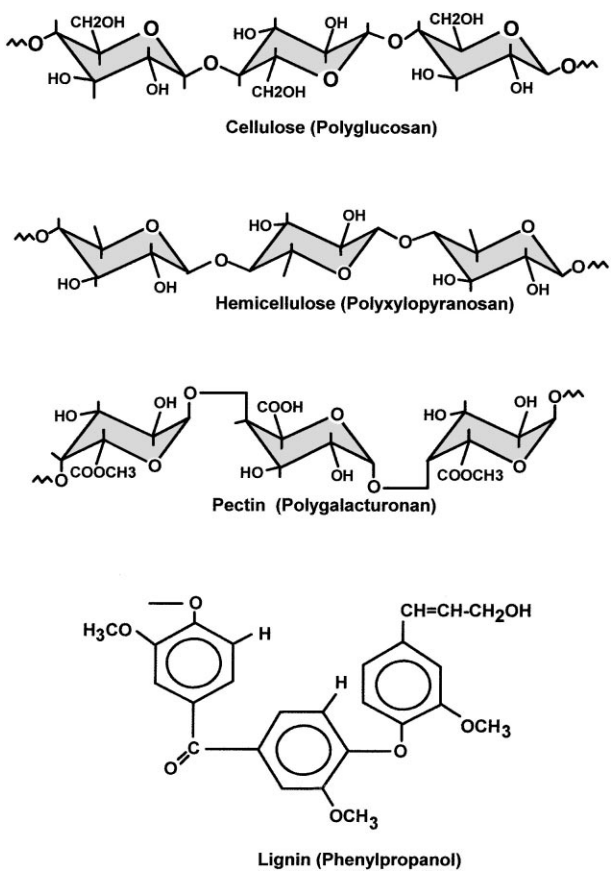

Fig. 5. Basic molecular structures of the major biopolymers forming the cell wall of wood: cellulose, hemicellulose, pectin and lignin.

quantity of acetyl esters. The most common uronic acid is D-galacturonic acid which is found in combination with D-galactose, L-arabinose, and L-rhamnose. Pectin is believed to have a higher degree of polymerization than hemicellulose, but still considerably below that of cellulose.

Lignin is an amorphous polymeric substance of high aromatic character but lack of regular periodic structural pattern characteristic of polymers in general. Lignin is a polymer of *p*-OH phenylpropanol that is linked in other repeat units in two dozen ways or more. Among intermonomer bonds are ether, ester, and carbon-to-carbon bonds, some fragile enough to allow the depolymerization of lignin to low-molecular-weight, alkali-soluble phenolic components (manufacturing of paper pulps). The structure of lignin has not been unequivovally established. The most prevalent concept considers it to be a three-dimensional highly branched polymer of unsaturated phenylpropane derivatives such as coniferyl- and sinapinal-alcohols with a variety of alkyl, hydroxyl, carboxyl, carboxymethyl, and methoxyl functional groups. It permeates cell walls and intercellular regions giving wood its relatively high hardness and rigidity. Lignin acts as a glue which bonds together all wood cells.

4. Conversion of lignocellulosics into ceramics

Conversion of lignocellulosics into ceramic products may start from native plant tissue or from preprocessed technical structures, e.g. delignified cellulose precursor

materials. Direct tissue reproduction generally deals with the problem of heterogeneity on the macro-, meso- and microscale levels of the naturally grown biostructure. Using preprocessed technical products such as paper, cardboards, matchwood, etc. may provide precursors which are homogeneous on the macroscale level, though the wood fibers are preferentially oriented perpendicular to the pressing or filtration direction applied during processing.

Converting native biopolymeric materials into non-oxide as well as oxide ceramic products includes: (i) high temperature pyrolytic decomposition resulting in a porous carbon replica (template) which may subsequently be reacted to form carbide phases or may be infiltrated with non-reacting sols or salts which can further be processed to yield oxide reaction products; (ii) low temperature infiltration with organometallic and metalorganic precursors followed by subsequent oxidation to remove free carbon phase. Fig. 6 shows a simplified road map of possible conversion reactions.

4.1. Carbon template formation

It has been demonstrated that net-shape ceramic composites can be produced using wood as a precursor. This was accomplished by controlled thermal decomposition to form a monolithic carbon template which retains the anatomical features of the precursor. Kinetics of thermally induced decomposition during pyrolysis are strongly affected by transport of gaseous decomposition products (H_2O, CO_2, and a variety of additional species) via the open pore channel system. The carbon template was shown to be easily machined to net shape prior to conversion to a ceramic composite.[25]

Mechanisms involved in conversion of cellulose to carbon are: (a) desorption of adsorbed water up to 150°C, (b) splitting off of cellulose structure water between 150 and 240°C, (c) chain scissions, or depolymerization, and breaking of C–O and C–C bonds within ring units evolving water, CO and CO_2 between 240 and 400°C, and (d) aromatization forming graphitic layers above 400°C. Heating of wood in inert atmosphere gives rise to the same products as would be given by the sum of its three major components pyrolyzed separately. Pyrolysis occurs in a stepwise manner with hemicellulose breaking down first at 200–260°C, cellulose next at 240–350°C and lignin at 280–500°C.[25] Between 200 and 400°C almost 80% of the total weight loss occurs which may vary between 40% (lignin) to about 80% (cellulose).

H_2O, CO_2, acids, carbonyl groups and alcohols are the volatile species whereas clusters and free radicals of carbon species are present in the residue. Simultaneously a pronounced anisotropic shrinkage was observed with 15–22% in axial and 22–40% in tangential (and radial) directions.[13] Between 400 and 800°C aromatic reactions occur and the carbon network shrinks to accommodate the excessive volume (vacancies) left by the evolving gases. Above 800°C thermal induced decomposition and rearrangement (condensation polymerisation) reactions are almost terminated leaving a carbon template structure. Residual hydrogen is released, defects are healed and the degree of crystallinity of the carbon units increases with temperature.

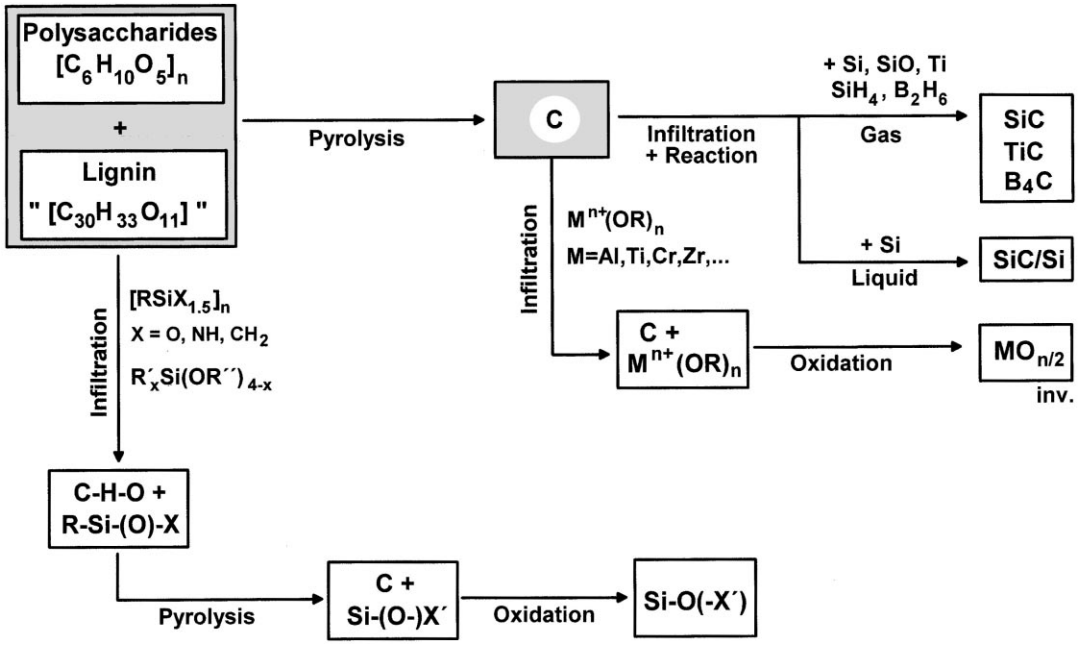

Fig. 6. Scheme of possible conversion reactions for ceramic manufacturing from wood.

Due to the high amount of oxygen present in cellulose no melt phase is formed upon pyrolysis and hence biocarbon residues derived from cellulose rich precursor tissues may not attain the full crystalline order (and density) of graphite. Only at temperatures above 1400°C small clusters of basic structural units (BSU).[27] were observed by TEM with average cluster sizes below 15 nm and stacking dimensions less than 4 nm at 1800°C.[13] Fig. 7 shows the basic molecular features of biopolymer to carbon conversion giving rise to a particular anisotropic structure of the carbon phase with a low degree of crystalline order.

Weight loss as well as linear shrinkage may vary tremendously depending on the composition and molecular structure of the wood tissue. Axial shrinkage increases with increasing misorientation angle of the cellulose macrofibrils in the cell wall segments. While in the pure cellulose fiber, formation of graphite-like planes parallel to the (101) plane of cellulose according to the longitudinal polymerisation model involving four carbon atoms (4-C-model) is expected to result in a theoretical shrinkage of 17% in fiber axis direction[28] higher shrinkage occurs when the fiber orientation deviates from the cell axis. Weight loss as well as shrinkage may be significantly reduced by triggering aromatisation reactions of the biopolymers via controlled oxidation,[29] adding $(NH_4)H_2PO_4$, $(NH_4)_2HPO_4$, $Na_2B_4O_7\times10H_2O$, NaCl[30] and applying slower heating rates which increases the char yield. If the four carbon residue theory, and the proposed theory of microfibril dominance are correct,[28] then a preferred orientation of graphitic crystallites should result from the highly oriented microfibril orientation particularly in cell wall layer S2. A simple relationship between density of precursor wood and that of carbonized wood is given.[25]

$$\rho_C = \Psi\rho_{wood} \tag{10}$$

where the constant Ψ depends on the particular carbonization conditions (T, P, t, A), and may attain values around 0.8.

4.2. Infiltration kinetics

The carbon template serves as a host for a fluid medium which either reacts with carbon to form a carbide phase or remains unreacted in the pore space. In any case infiltration of the porous precursor structure with the fluid medium is necessary. Based on Navier–Stokes relations for hydrodynamic systems capillary flow for a stationary current of an incompressible fluid with constant viscosity η may be expressed by[31]

$$\nabla^2\dot{h} = \frac{1}{\eta}\nabla p \tag{3}$$

where $\dot{h}$ is the infiltration rate (e.g. height h after time t, $\dot{h} = dh/dt$) and ∇p denotes the effective pressure gradient driving the infiltration process. In the absence of an external pressure infiltration dynamics of liquids into

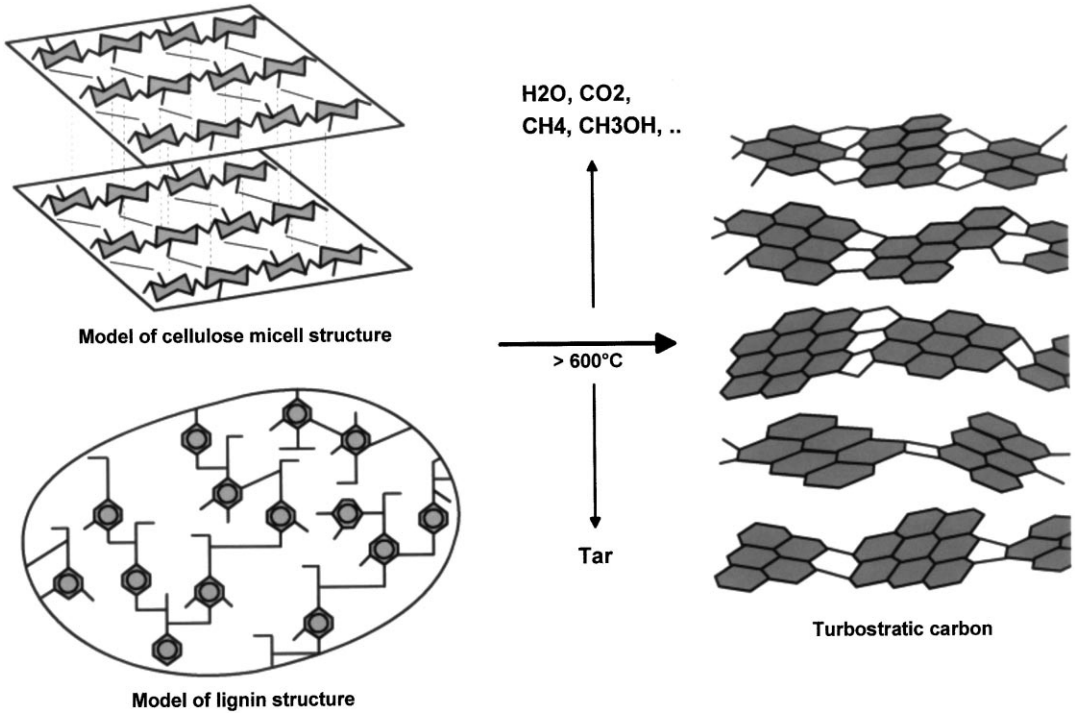

Fig. 7. Model of structural transition during pyrolysis from wood to carbon.

porous compacts is driven by capillary forces which are balanced by frictional and inertia forces. In a system of cylindrical capillaries of initial diameter d_{c0} time dependent height of infiltration perpendicular to gravity g follows the fundamental relations of Hagen and Poiseuille[32] which are expressed by a non-linear differential equation

$$\frac{32\eta}{d_{c0}^2}h(t)\dot{h}(t) + \rho_l g h(t) - \frac{4\gamma\cos\varphi}{d_{e0}} = 0 \tag{4}$$

where φ is the contact angle of liquid on solid and ρ_l is the liquid density. Integrating Eq. (4) gives[33]

$$t = \frac{32\eta}{d_{c0}^2\rho_l/g}\left(h_{max}\ln\frac{h_{max}}{h_{max}-h} - h\right) \tag{5}$$

with the maximum infiltration height h_{max} limited by

$$h_{max} = \frac{4\gamma\cos\varphi}{d_{c0}\rho_l g} \tag{6}$$

For the case of silicon carbide formation via liquid silicon infiltration (ρ_l at 1420°C is 2.53–2.55 g/cm^3 surface tension γ is 0.72–0.75 N/m at 1550°C; wetting angle φ is 0–22° on carbon in vacuum and 30–40° on SiC; viscosity η is 5.1–7.65×10^{-4} Pas at 1440°C) into the biocarbon template, infiltration time is in the range of seconds to minutes for reasonable template geometries, Fig. 8.

Taking into account an interface reaction between the liquid and the carbon, the effective flow diameter is changed according to[34]

$$d_{ce} = d_{c0} - 0.64\sqrt{\frac{2DM\rho_l t}{M_l}} \tag{7}$$

where M and M_l are the molecular weights of SiC and Si (l), respectively, and D is the effective diffusion coefficient governing the SiC growth rate [$D = D_0\exp(-E/RT)$ with $D_0 = 2\times10^{-10}$ (m^2/s) and $E = 132$ [kJ/mol]].[35] Estimation of infiltration times versus reaction times suggests the infiltration to be several order of magnitudes faster than the reaction and hence the reaction is supposed to be the time limiting step in the liquid infiltration process. For the case of capillary wetting without applying an additional external pressure a maximum capillary diameter, d_{cmax} limits spontaneous infiltration perpendicular to the fluid surface

$$d_{cmax} \approx \frac{4\gamma\cos\varphi}{\rho g h} \tag{8}$$

For liquid Si infiltration a d_{cmax} of 120–80 μm was found.[4]

Instead of liquid media gaseous infiltrants can be used to convert the lignocellulosics precursor into ceramic phases. The attainable impregnation depth is one of the most important criteria for massive in-pore deposition and reaction. Penetration depth h for cylindrical pores is

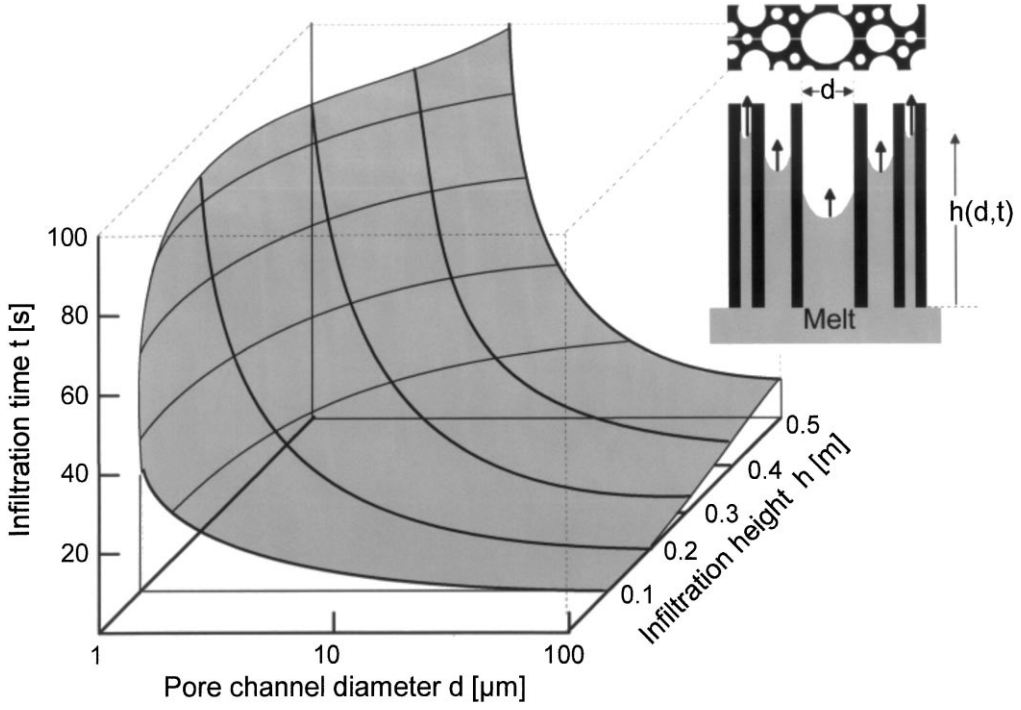

Fig. 8. Infiltration time as a function of pore channel diameter and infiltration height for liquid silicon infiltration calculated according to Eq. (5).

given as a function of the temperature dependent rate constant α by[36]

$$h = \phi\sqrt{\frac{d_c D_{eff}}{4\alpha}} \quad (9)$$

where ϕ is the Thiele modulus, which typically is used to describe the relative rates of reaction and diffusion in a porous body. For the case that diffusion is fast and hence adsorption and reaction at the carbon-infiltrant interface is rate controlling $\phi < 0.1$. The effective diffusion coefficient D_{eff} is given by

$$\frac{1}{D_{eff}} = \frac{\tau}{\varepsilon}\left(\frac{1}{D_{mol}} + \frac{1}{D_{Knu}}\right) \quad (10)$$

ε is the porosity of the template (0.5–0.8) and τ represents the tortuosity (3 for cylindrically shaped pores). While for unconstrained molecular gas transport D_{mol} of a gas species of molecular size Ω and molecular mass M is independent of pore size

$$D_{mol} = \left(\frac{kT}{\pi}\right)^{3/2}\left[\Omega^2\sqrt{M}p\right]^{-1} \quad (11)$$

Knudsen diffusion at small pore sizes depends on pore channel diameter

$$D_{Knu} = \left(\frac{2d_p}{3}\right)\sqrt{\frac{2kT}{\pi M}} \quad (12)$$

resulting in significantly reduced penetration rates. Thus, a lower critical pore channel diameter may be derived from the condition $D_{mol} = D_{Knu}$

$$d_{cmin} = \frac{6kT}{\pi\Omega^2 p} \quad (13)$$

below which no effective gas phase transport can occur within reasonable time. Estimation of d_{cmin} for gas phase infiltration with Si and SiO at 1400–1600°C, Fig. 9, suggested a critical pore channel diameter in the range of 1 μm.[13] Thus for both kinds of infiltration via liquid or gaseous media, pore diameters larger than 1 μm are required to obtain reasonable infiltration rates.

4.3. Conversion of the carbon template into ceramic

Infiltration and reaction with liquid Si or gaseous Si and SiO were used to form β-SiC pesudomorphous to wood tissue[4,37]

$$C_{Bio} + Si(l) \rightarrow \beta\text{-SiC} \quad (14)$$

$$C_{Bio} + Si(g) \rightarrow \beta\text{-SiC} \quad (15)$$

$$2\ C_{Bio} + SiO(g) \rightarrow \beta\text{-SiC} + CO \quad (16)$$

$$3\ C_{Bio} + 2\ SiO(g) \rightarrow \beta\text{-SiC} + CO_2 \quad (17)$$

Reaction (14) results in SiC/Si composite ceramics with a residual Si content in cellular pores smaller than approximately 30 μm.[4] SiC formation using gaseous reactants according to Eqs. (15)–(17) results in a single phase SiC material. While reactions (15) and (17) involve a specific volume increase of +108 and +39%, respectively, reaction (16) is associated with a volume change of only +4%. In the presence of oxygen reaction (17) dominates at lower temperatures whereas reaction (16) prevails at temperatures above 1400–1500°C. Fig. 10 shows the cellular pore structure of oak converted to β-SiC by gas phase reaction (16).

Correlation of final pore size in SiC with the initial cell wall thickness t and cell diameter d_c of the wood tissue may serve as a guideline for selection of suitable kinds of wood which allow the fabrication of cellular ceramics with tailored pore microstructure. Fig. 11 shows a pore size selection map taking into account the specific volume changes upon pyrolysis and reaction. As may be seen, average pore sizes of most cellular SiC ceramics manufactured from the majority of woods by gas phase reaction (16) should lie in the range of 10–100 μm. Increasing cell wall thickness may account for SiC struts of corresponding thickness which are expected to exhibit higher strength compared to cellular ceramics of smaller strut thickness.

Alternatively, the porous carbon template can be infiltrated with oxide precursor solutions such as TEOS ($Si(OC_2H_5)_4$), metal salts of organic acids such as acetates, oxalates, etc. and subsequently converted to the carbidic reaction product. The residual carbon network is removed by oxidation in air leaving an inverted metal oxide structure of the initial tissue anatomy. Upon infiltration with a sodium chloride melt at 800°C and subsequent removal of the carbon template by oxidation at 600°C, the pore space may be refilled by an oxidic precursor sol. After leaching of the salt and final calcination in air an oxidic reproduction of the initial tissue may be obtained.

4.4. Direct infiltration and conversion reaction

It has been stated that the matrix of the woody cell wall e.g. hemicellulose and lignin, is the major contributor of sorption capacity to the cell wall. Although the chemical structure of cellulose contains many hydroxyl groups, the crystalline nature of cellulose may render the groups largely unavailable for either sorption of water or reaction with chemicals such as acetic anhydride or isocyanate.[37] Low temperature processing avoiding formation of a carbon template by pyrolysis treatment involves infiltration of the native tissue with monomeric, oligomeric or polymeric precursor compounds based on $Si(OR)_4$, $R'_xSi(OR'')_{4-x}$, or $[R_2SiX]_n$ with X = O (siloxanes), NH (silazanes), CH_2, (carbosilanes), etc. Due to the chemical coupling with the

hydroxyl groups of the glucose units, weight loss and shrinkage upon subsequent heat treatment may be reduced. After pyrolysis, final oxidation in air results in a silicon containing Si–O(–X) material of high porosity. Using infiltrants loaded with metallic filler particles reaction of the carbon network to form a carbide phase may be used to form interpenetrating network composite materials. Impregnation of the surface of dried wood with low viscous preceramic polymer solutions and subsequent conversion to a ceramic residue by local heating (e.g. laser pyrolysis) of the surface finally results in novel kinds of ceramic-wood gradient materials. While the bulk

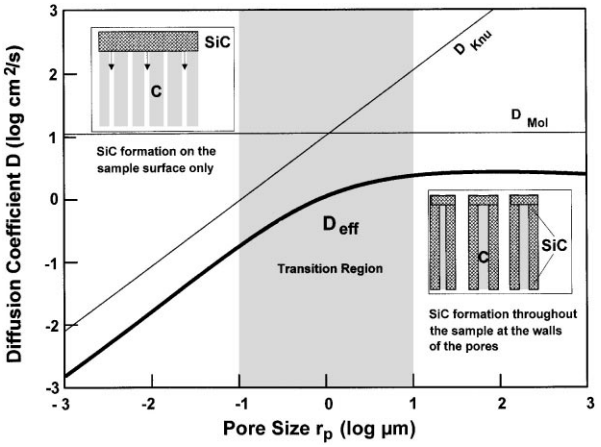

Fig. 9. Effective diffusion coefficient of SiO (g) as a function of the pore channel diameter for gas phase infiltration.

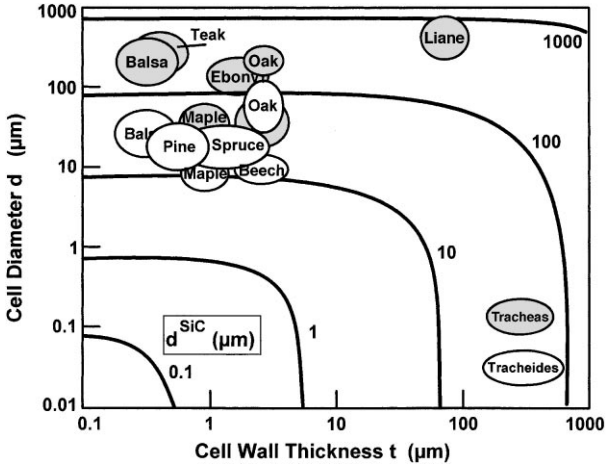

Fig. 11. Pore size selection map showing the resulting pore diameter of gas phase reacted β-SiC ceramic as a function of initial pore microstructure in wood.

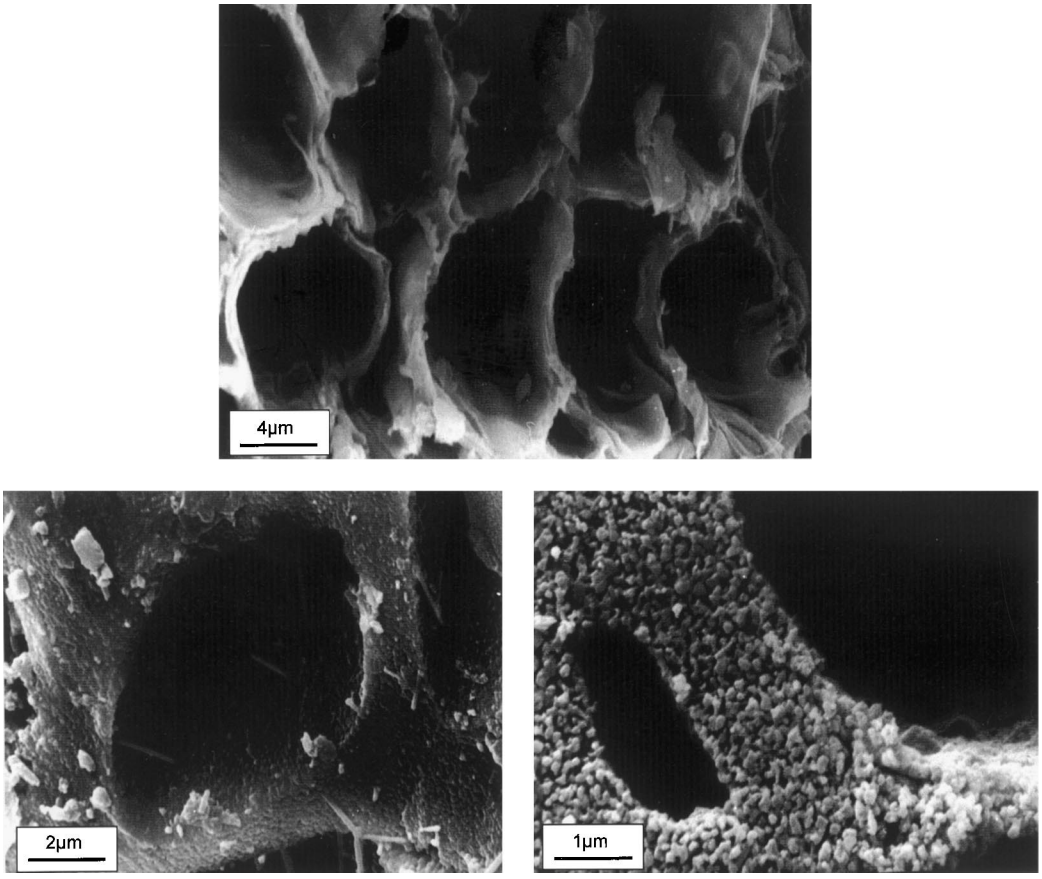

Fig. 10. Porosity microstructure of gas phase reacted β-SiC pseudomorphous to oak.

still remains as native wood, the ceramic surface offers a significantly improved wear resistance and strength.

5. Applications of biomorphous ceramics

Fig. 12 shows principal cellular structures which may be derived from native plants. Ceramics with a *homogenous porosity structure* are possible candidates for filter, catalyst carrier, aerator structures, etc. Filter structures require a well defined monomodal pore size to provide a cut off dimensional limit necessary for filter selectivity. Due to the specific cell microstructure of naturally grown traeidal tissue, small pores in the cell walls offer the possibility to provide gas flow between the large cellular pores e.g. a high permeability perpendicular to the major filtering direction. Porous devices with permeable struts can be used as irrigators in the agriculture industry. Multifunctional ceramic membrane reactors (CMRs) is another field of potential application. Perm- and non-perm-selective catalytically active membranes surrounded by a bed of catalyst particles have become of importance for gas separation (H_2 from CO and CO, formed by steam reforming of CH_4), O_2–N_2 separation for pure O_2-production from air, dehydrogenation and dehydration reactions (of ethane, propane, cylohexane, ethylbenzene), catalytic partial oxidation of CH_4 to syn-gas for methanol production, etc. While tubular membranes provide a surface to volume ratio of <4000 l/m, surface to volume ratio in cellular ceramics manufactured by gas phase reaction of oak attains more than 10^6 l/m.

Ceramics derived from parenchymal tissue could find applications as catalyst carrier and fluid/gas reservoir devices. Due to the irregular star-like strut anatomy, turbulent flow is favoured in these structures which may cause prolonged reaction time for surface-coated catalysts. Thus, design of appropriate catalyst structures may be improved with respect to fluid dynamics, size, pressure drop, etc. This could be interesting for miniaturized reactor devices to be used in chemical reaction technology (pharmaceutical production biotechnology).

Cellular ceramics from *heterogeneous tissue* are interesting materials for the design of multifunctional cell carrier and biocatalyst support structures. Multimodal pore size structures as biocatalyst supports could find applications in the food industry, fermentation or waste water treatment. Fig. 12 shows a possible lay-out of an advanced microreactor substrate with large tubular pores for transport of media and small pores where the catalytically active bio-organisms are fixed. Immobilization of microbes of enzymes requires accessible pore sizes of 10–500 μm. Cell carriers with an open pore structure may become interesting for ex vivo molecular biological cell reactor systems as well as artifical organs in medicine. Large pores with a diameter in the range of 100–500 μm provide the transportation system for nutrients and metabolisms whereas the cells are located in the pores smaller than 100 μm. Use of multimodal pore sizes or fractal pore distributions offer the possibility of simultaneous operation of different kinds of cells which differ significantly in the required pore space.

Recently, the power-law behavior of transport properties at low wetting phase saturations has been related to the thin-film physics of the wetting phase and the fractal character of the pore space of natural porous media.[38] The power law deduced for the electrical

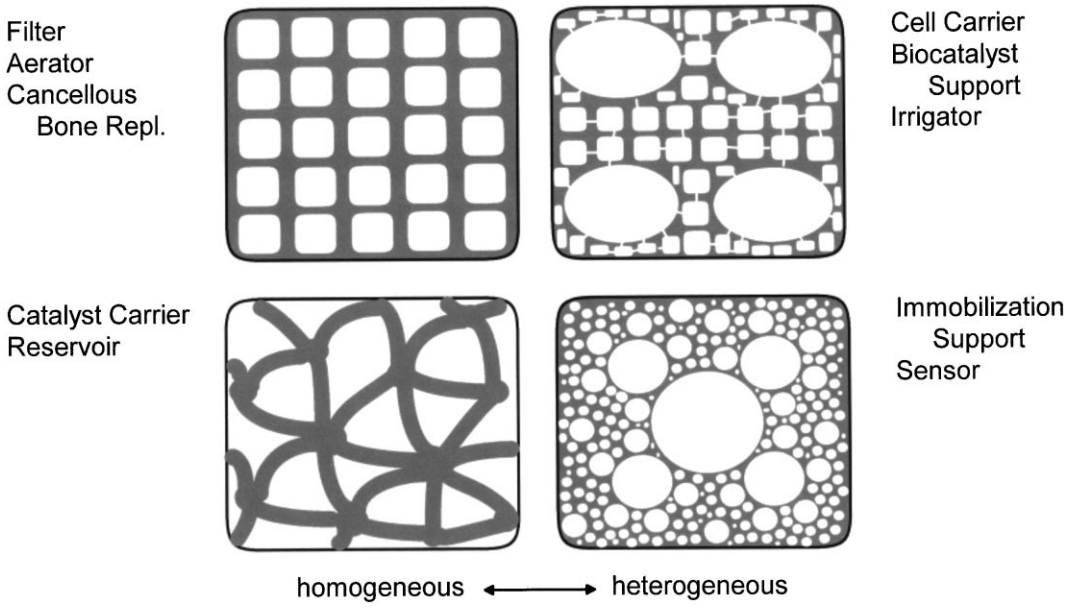

Fig. 12. Potential fields of application for biomorphous ceramics with uniform and non-uniform porosity micro structures.

conductivity σ as a function of the degree of saturation S_w, for example, is given by

$$\sigma = CS_w^{\left(\frac{1}{m(2-D)}\right)} \quad (18)$$

C is a constant and D is the fractal dimension. m is an exponent which represents the specific interaction mechanism (e.g. $m = 1$ for short range structural forces, $m = 2$ for electrostatic interaction and $m = 3$ for van der Waals forces). Fractal porosity may, therefore, be of interest for design of novel kinds of sensor structures. At low saturation levels (e.g. S_w, $< 10\%$), electrical conductivity varies with the degree of saturation with a significantly higher sensitivity ($D = 2$ ...3) compared to monomodal porosity distribution ($D = 1$).

6. Conclusions

Native or preprocessed lignocellulosics may be successfully used as a template for generating ceramic materials pseudomorphous to the initial cellular structure. Depending on the wide variety of native wood structures ceramics with a uniform as well as non-uniform (hierarchical) pore structure can be processed. The resulting cellular ceramics, which might be called ''lignocers'', are generally characterized by a highly anisotropic microstructure giving rise to anisotropic material properties. Based on rapid fluid infiltration into the accessible cellular template structure a variety of chemical processing routes offer a wide range of chemical compositions and structural modifications in the ceramic reaction products. Making use of the unique fibrillar cell wall architecture and the hierarchical porosity structure novel cellular ceramics derived from readily available lignocellulosics might be of interest for high temperature resistant exhaust gas cleaning devices, advanced microreactor systems, immobilization supports for medical and biotechnological processes, etc..

Acknowledgements

Financial support from Volkswagen-Foundation is gratefully acknowledged.

References

1. Glasser, W. A., Chemical products from lignocellulosics. *Mat. Res. Soc. Bull.*, 1994, **19**, 46.
2. Li, H., Zeng, Q. Y., Ziao, Y. L., Fu, S. Y. and Zhou, B. L., Biomimicry of bamboo bast fiber with engineering composite materials. *Mat. Sci. Eng.*, 1995, **C3**, 125.
3. Ota, T., Takahashi, M., Hibi, T., Ozawa, M. and Suzuki, H., Biomimetic process for producing SiC wood. *J. Am. Ceram. Soc.*, 1995, **78**, 3409.
4. Greil, P., Lifka, T. and Kaindl, A., Biomorphic cellular silicon carbide ceramics from wood: I. Processing and Microstructure; II. Mechanical Properties. *J. Eur. Ceram. Soc.*, 1998, **18**, 1961–1975.
5. Shin, D. W. and Park, S. S., Silicon/silicon carbide composites fabricated by infiltration of a silicon melt into charcoal. *J. Am. Ceram. Soc.*, 1999, **82**, 3251.
6. Nienhuis, C. and Barthlott, W., Characterization and distribution of water-repellent, self-cleaning plant surfaces. *Annals of Botany*, 1997, **79**, 667.
7. Patel, M. and Padhi, B. K., Production of alumina fibre through jute fibre substrate. *J. Mat. Sci.*, 1990, **25**, 1335.
8. Patel, M. and Padhi, B. K., Titania fibres through jute substrates. *J. Mat. Sci. Lett.*, 1993, **12**, 1234.
9. Krishnaro, R. V. and Mahajan, Y. R., Preparation of silicon carbide and silicon nitride fibres from cotton fibre. *J. Mat. Sci. Lett.*, 1996, **15**, 232.
10. Sharma, N. K. and Williams, N. S., Formation and structure of silicon carbide whiskers from rice hulls. *J. Am. Ceram. Soc.*, 1984, **67**, 715.
11. Patel, M. and Karera, A., SiC Whiskers from rice husk: role of catalysts. *J. Mat. Sci. Lett.*, 1989, **8**, 955.
12. Singh, S. K., Stachowicz, L., Girshick, S. L. and Pfender, E., Thermal plasma synthesis of sic from rice hull. *J. Mat. Sci. Lett.*, 1993, **12**, 659.
13. Kaindl, A., Cellular SiC Ceramics from Wood, PhD thesis, University of Erlangen-Nuernberg (2000) (in German).
14. Wagenführ, R., HOLZatlas, Fachbuchverlag Leipzig (1996) (in German).
15. Gibson, L. J. and Ashby, M. F., *Cellular Solids, Structure and Properties*. Pergammon Press, New York, 1988.
16. Gibson, L. J., Wood: a natural fibre reinforced composite. *Metals and Materials*, 1992, **8**, 333.
17. Panshin, A. J. and deZeeuw, C., *Textbook of Wood Technology*. McGraw-Hill, New York, 1980.
18. Lucas, P. W., Darvell, B. W., Lee, P. K., Yuen, T. B. D. and Choong, M. F., The toughness of plant cell walls. *Phil. Trans. Roy. Soc. Lond.*, 1995, **B348**, 363.
19. Eschrich, W., *Funktionelle Pflanzenanatomie*. Springer Verlag, Berlin, GE, 1005.
20. Lachaud, S., Participation of auxin and abscisic acid in the regulation of seasonal variations of cambial activity and xylogenesis. *Trees*, 1989, **3**, 125.
21. Higuchi, T., Biochemistry and molecular biology of wood. *Springer Series in Wood Science*, Springer Verlag, Berlin, 1997.
22. Bauer, T. and Eschrich, W., Mechanical pressure inhibits vessel development of xylogenic cambial derivatives of beech (*Fagus sylvatica* L.). *Trees*, 1997, **11**, 349.
23. Atalla, R. H. and Hackney, J. M., Structural polysaccharides in molecular architecture of plant cell walls — from algae to hardwoods. *Mat. Res. Soc. Symp.*, Vol. **255**, Mat. Res. Soc., Pittsburgh, PE, 1992 p. 387.
24. Rebenfeld, L., Hierarchical structure and physical properties of natural cellulosic fibers, *Mat. Res. Soc. Symp.*, Vol. **255**, Mat. Res. Soc., Pittsburg, PE, 1992 p. 399.
25. Byrne, C. E. and Nagle, D. C., Carbonization of wood for advanced materials applications. *Carbon*, 1997, **35**, 259.
26. Vinvcent, J. F. V., *Structural Biomaterials*. John-Wiley Sons, New York, 1982.
27. Oberlin, A., Carbonization and graphitization. *Carbon*, 1984, **22**, 521.
28. Bacon, R. and Tang, M. M., Carbonization of cellulose fibers. *Carbon*, 1964, **2**, 211.

29. Norton, F. J., Love, G. D., Mackinnon, A. J. and Hall, P. J., Mechanisms of char production from oxidized cellulose. *J. Mat. Sci*., 1995, **30**, 596.
30. Shafizadeh, F. and Sekiguchi, Y., Development of aromaticity in celluosic chars. *Carbon*, 1983, **21**, 511.
31. Happel, J. and Brenner, H., *Low Reynolds number hydrodynamics*. Martinus Nijhoff, Dordrecht, NE, 1983.
32. Schade, H. and Kunze, E., *Strömungslehre*. Walter de Gruyter, Berlin, 1980.
33. Levich, V. G., *Physicochemical Hydrodynamics*. Pentice Hall, Englewood Cliffs, NJ, 1962.
34. Gern, F. H., Capillary and infiltration behavior of liquid silicon impregnation of carbon/carbon components, Res. Report DLR 95-25, Deutsches Zentrum für Luft- und Raumfahrt, Köln, 1995 (in German).
35. Gadow, R., Die Silicierung von Kohlenstoff, PhD thesis University of Karlsruhe, 1986 (in German).
36. Geiger, G. H. and Poirier, D. R., *Transport Phenomena in Metallurgy*. Addison-Wesley, New York, 1980.
37. Vogli, E., Mulcherji, J., Hoffmann, C., Kladny, R., Siber, H., Greil, P., Conversion of oak to cellular silicon carbide ceramic by gas phase reaction with SiO. *J. Am. Ceram. Soc*., 2001, in press.
38. Araujo, Y. C., Toledo, P. G. and Gonzalez, H. Y., Scaling of transport properties of reservoir material at low saturations of a wetting phase. *Mat. Res. Soc. Symp. Proc*. Vol. 367, Mat. Res. Soc., Pittsburgh, PE, 1995 p. 255.